Information processing second law for an information ratchet with finite tape

Lianjie He, Andri Pradana, Jian Wei Cheong, and Lock Yue Chew*

Division of Physics and Applied Physics, School of Physical and Mathematical Sciences, Nanyang Technological University, 21 Nanyang Link, Singapore 637371, Singapore

(Received 15 January 2022; revised 19 April 2022; accepted 3 May 2022; published 23 May 2022)

We model a class of discrete-time information ratchet with a *finite* tape and explore its thermodynamic consequence as a Maxwell demon. We found that, although it supports the operational regime of an engine or eraser, it cannot typically sustain these thermodynamic functionalities due to eventual equilibration as a result of the finite information capacity of the tape. Nonetheless, cumulative work can be accrued or expended through successive tape scans and we prove that at all time the ratchet obeys the information processing second law (IPSL). Unlike the IPSL for the infinite-tape ratchet which operates only at the stationary state, the IPSL here is applicable also at the transient phase of the ratchet operation. We explore two ratchet designs with the single-state perturbed coin (PC) ratchet being the simplest ratchet without memory, while the double-state modified Boyd's (MB) ratchet is the simplest ratchet with memory. Our analysis shows that the MB ratchet can harness correlation to accumulate more work by having a larger time constant to reach steady state relative to the PC ratchet.

DOI: 10.1103/PhysRevE.105.054131

I. INTRODUCTION

Purportedly a violation of the second law of thermodynamics by Maxwell, his eponymous demon had initially baffled physicists who sought to overcome its challenge to the paradigm prescribed by classical thermodynamics [1,2]. Notwithstanding the eventual resolution by Landauer [3] and Szilard [4] that heat dissipation is inevitable with information erasure, it had generated new insights in this burgeoning field at the intersection between information science and statistical physics [5–8]. A critical knowledge of this new understanding will not only augment existing theoretical frameworks [9–17], but also pave the way for the next generation of computer processors dominated by miniaturization at the nanoscale [18–22].

The literature presents various approaches to conflate information theory and thermodynamic principles, and can be broadly classified into two distinct classes. The measurement-feedback formalism is the first approach expounding on the ideas of Maxwell and Szilard by performing an explicit measurement on the system under consideration whose instantaneous outcome determines its parameters to be altered [23–25]. The act of measurement drives the system away from equilibrium and governs its subsequent evolution. In this description, Sagawa and Ueda have established an integral fluctuation theorem whose corresponding inequality bounds the extracted work, originated as heat from a coupled heat bath, by the information acquired in the preceding measurement [26,27]. This perspective thus generalizes the second law to such systems operating on feedback-driven schemes. The second approach utilizes a tape with an infinite sequence of symbols or *bits* to interact with the system. It seeks to replicate the dynamics of an *autonomous* information ratchet similar to that in the earlier treatment but now accounting for the previously absent thermodynamic costs accrued by measurement and information erasure [28,29]. In this framework, a similar inequality was derived where the single-symbol Shannon entropy difference between outgoing and incoming tape is an upper bound for the maximal rate of work extraction. The model described deals with stochastic transitions spanning continuous time but there exist analogs for discrete time.

This paper considers an information ratchet that interacts with a finite length of symbol or bit sequence in discrete time solely from the perspective of a fully *autonomous* Maxwell demon with no external agent manipulating it or explicit thermodynamic force driving it, adopting the second approach introduced earlier in [28,29]. Such a finite sequence constitutes a finite tape which relaxes from being an information reservoir of the original discrete-time information ratchet with an infinite bit sequence [30]. Moreover, the finite tape opens up the possibility of recycling the output tape with repeated *tape* scans by the information ratchet (i.e., preceding output sequence is the input sequence in the immediate scan). It provides a paradigm for the realization of a more physically realistic ratchet system with the promised behaviors of engine or eraser. Attempts to make the tape-ratchet system more realistic had also been achieved with a model of a *thermal tape* [31].

The organization of our paper is as follows. We first introduce the setup for an information ratchet with a finite tape before giving details to its mathematical formulation. We then prove the information processing second law (IPSL) for it in terms of the extracted work and its upper bound. We then proceed to demonstrate two designs of this finite-tape information ratchet. One design is based on the perturbed coin (PC) [32,33], while the other is a modification of Boyd's (MB) information ratchet [30,32,34]. Our choice of design is

*lockyue@ntu.edu.sg

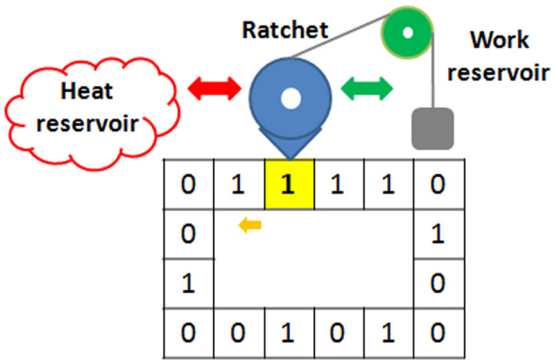

FIG. 1. Schematic representation of an information ratchet with the finite tape moving unidirectionally (indicated by arrow below the bit highlighted in yellow) as it sequentially interacts with each bit successively; the bit highlighted in yellow is the current bit B_N interacting with the ratchet.

simplicity, where the former and the latter are the simplest information ratchets with and without memory, respectively.

II. INFORMATION RATCHET WITH FINITE TAPE

An information ratchet can be perceived as a channel mediating exchanges between the heat, work, and information reservoirs. The heat and work reservoirs have their usual interpretations from classical thermodynamics, with the latter arbitrarily perceived as a mass-pulley system which stores (expends) work as the mass is raised (lowered). Instead of an information reservoir with an infinite sequence of bits with values of 0 or 1 as depicted in other information ratchet systems, our information ratchet interacts with a tape that stores a finite string of 0 or 1. Figure 1 gives a diagrammatic representation of the processing of a bit stream by the finite-tape information ratchet, with R_N and B_N the random variables for the ratchet state and bit state, respectively, at time step $N\tau$. The tape moves unidirectionally (counterclockwise in Fig. 1) as the ratchet (fixed spatially) sequentially interacts with each input bit successively for a fixed period τ. At the start of a cycle, the ratchet is initially not attached to any bit before the incoming input bit B_N attaches to it. This bit B_N of the tape is the current bit attached to and interacts with the ratchet via thermal transitions stochastically governed by a Markovian dynamic [30,32,34,35]. Next, the output bit B'_N from this (*bit* scan) interaction detaches from the ratchet and it shifts to the left of the ratchet, completing the cycle. We note that the specific points of onset of attachment and detachment of the individual bits to the ratchet do not involve any net energy flow between the interacting bit-ratchet subsystem and the reservoirs, and also the distributions of B_N and R_N are unchanged. The start and end instances of this attachment and detachment mechanism do not play a role in the energetics or informational change within the cycle but manifest as an intrinsic feature of this information ratchet necessary for the sequential interaction of each bit with the ratchet.

We will now present the mathematical formalism to model this ratchet operation described above.

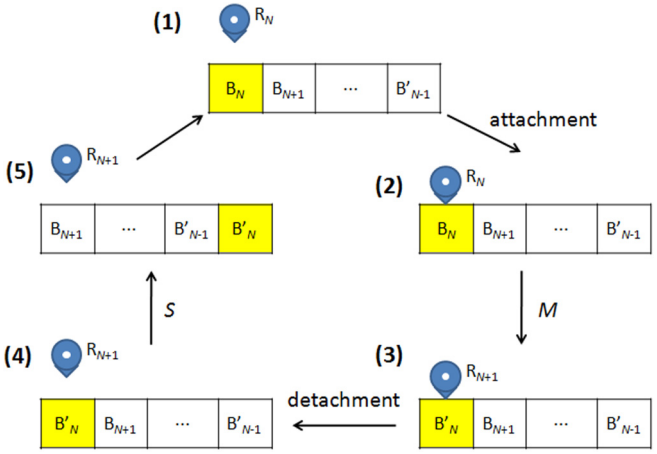

FIG. 2. Schematic representation of a single *bit* scan operation O with the intermediate stages detailing the coupling between the interacting bit B_N and the ratchet R_N, taking into account the position of B_N (and subsequently B'_N) relative to the other bits in the finite tape of length L. The linear tape here corresponds to the circular tape in Fig. 1 and is presented in a different but physically equivalent manner; the bit highlighted in yellow in Figs. 1 and 2 is the same bit B_N.

III. MATHEMATICAL FORMALISM FOR FINITE-TAPE INFORMATION RATCHET

We present the previous circular tape (Fig. 1) in a linear fashion in Fig. 2, where we arbitrarily take the forward direction spatially in which the tape is scanned as the left-to-right direction in this paper hereafter. In our proposed framework, we characterize the joint tape-ratchet states of the information ratchet *system* by the probability distribution $\mathbf{p}$. The consideration of joint tape-ratchet states would capture the statistical behavior of all the microstates of this (tape-ratchet) system. For an information ratchet with N_R ratchet states and a tape of L bits, $\mathbf{p}$ is a $2^L N_R \times 1$ vector. The ratchet itself (with N_R ratchet states) interacting with the L-bit tape constitute our information ratchet (tape-ratchet) system. The memory capacity of this system is thus attributed to the ratchet itself with a memory of $\log_2 N_R$ bits and the L-bit tape with its memory of L bits.

We employ the operator matrix O to evolve $\mathbf{p}$, which mathematically models a single *bit* scan, and successive operations reflect the ratchet operation mechanism where each bit interacts with the ratchet sequentially. In Fig. 2, note that the attachment (from stage 1 to 2) and detachment (from stage 3 to 4) of bits to the ratchet only facilitate this ratchet mechanism and have no bearing on the energy or informational flow in a cycle O. Other processes involved in this cycle are the thermal transition M and switching operation S required to move the output bit from the leftmost end of tape to the right end as modeled by the linear tape. Each *bit* scan thus effectively constitutes a two-step process of thermal transition M followed by switching S, which can now be perceived as a *composite* operation $O = SM$.

The matrix M accounts for a stochastic transition of the bit-ratchet state due to thermal excitation. After the operation M, the interacting leftmost bit of the tape transforms to

an output bit that remains in position at the left end of the tape, signifying its continued physical attachment with the ratchet and corresponds to the transformation from stage 2 to 3 in Fig. 2. To exemplify this operation, let us consider a single-state ratchet $N_{\mathrm{R}} = 1$ here for clarity. For $L = 1$, the left stochastic transition matrix corresponding to this thermal transition step M is

$$M_{1\text{-bit}} = \begin{array}{c} \\ 0 \\ 1 \end{array} \begin{array}{c} \begin{array}{cc} 0 & 1 \end{array} \\ \left(\begin{array}{c|c} \times & \times \\ \hline \times & \times \end{array}\right) \end{array} = \left(\begin{array}{c|c} E & F \\ \hline G & H \end{array}\right), \tag{1}$$

with $\times$ denoting the respective transition probabilities. Note that the ratchet state in the joint tape-ratchet state labels at the top and side of the matrix in Eq. (1) has been omitted without compromising the ensuing discussion. For this $N_{\mathrm{R}} = 1$ ratchet with 2-bit tape,

$$M_{2\text{-bit}} = \begin{array}{c} \\ \underline{0}0 \\ \underline{0}1 \\ \underline{1}0 \\ \underline{1}1 \end{array} \begin{array}{c} \begin{array}{cccc} \underline{0}0 & \underline{0}1 & \underline{1}0 & \underline{1}1 \end{array} \\ \begin{pmatrix} \times & \times & \times & \times \\ \times & \times & \times & \times \\ \times & \times & \times & \times \\ \times & \times & \times & \times \end{pmatrix} \end{array}, \tag{2}$$

where the only bit involved in this thermal transition is the leftmost attached bit and underlined for emphasis. Note that the labels of the joint tape-ratchet state at the top of the matrix are the input and that at the side of the matrix correspond to the output.

In general, E, F, G, and H are $N_{\mathrm{R}} \times N_{\mathrm{R}}$ submatrices of the 1-bit tape transition matrix $M_{1\text{-bit}}$ for arbitrary N_{R} and ratchet design since only the leftmost bit is coupled to the ratchet and can undergo transitions governed by this $M_{1\text{-bit}}$. Correspondingly,

$$M_{2\text{-bit}} = \left(\begin{array}{cc|cc} E & & F & \\ & E & & F \\ \hline G & & H & \\ & G & & H \end{array}\right) = \begin{pmatrix} \mathbb{1}_2 \otimes E & \mathbb{1}_2 \otimes F \\ \mathbb{1}_2 \otimes G & \mathbb{1}_2 \otimes H \end{pmatrix}, \tag{3}$$

$$M_{L\text{-bit}} = \begin{pmatrix} \mathbb{1}_{2^{L-1}} \otimes E & \mathbb{1}_{2^{L-1}} \otimes F \\ \mathbb{1}_{2^{L-1}} \otimes G & \mathbb{1}_{2^{L-1}} \otimes H \end{pmatrix}, \tag{4}$$

with $\mathbb{1}_2 = \left(\begin{smallmatrix} 1 & 0 \\ 0 & 1 \end{smallmatrix}\right)$ the 2×2 identity matrix.

For $L > 1$, the (underlined) output bit does not immediately interact with the ratchet in the next *bit* scan. The switching step S is required to switch this (now detached) leftmost output bit from the preceding thermal transition M to the right end of the tape before the ratchet is ready to attach to the next input bit, i.e., stage 4 to 5 in Fig. 2. With the $N_{\mathrm{R}} = 1$ ratchet, the required operation is

$$S_{2\text{-bit}} = \begin{array}{c} \\ \underline{0}0 \\ \underline{0}1 \\ \underline{1}0 \\ \underline{1}1 \end{array} \begin{array}{c} \begin{array}{cccc} \underline{0}0 & \underline{0}1 & \underline{1}0 & \underline{1}1 \end{array} \\ \begin{pmatrix} 1 & 0 & 0 & 0 \\ 0 & 0 & 1 & 0 \\ 0 & 1 & 0 & 0 \\ 0 & 0 & 0 & 1 \end{pmatrix} \end{array}, \tag{5}$$

where the interacted bit in the prior thermal transition (underlined above) has been shifted from the leftmost to rightmost end of tape. Similarly, it can be compacted to

$$S_{2\text{-bit}} = \left(\begin{array}{cc|cc} 1 & 0 & 0 & 0 \\ 0 & 0 & 1 & 0 \\ 0 & 1 & 0 & 0 \\ 0 & 0 & 0 & 1 \end{array}\right) = \left(\begin{array}{c|c} \mathbb{1}_2 \otimes \begin{bmatrix} 1 \\ 0 \end{bmatrix} & \mathbb{1}_2 \otimes \begin{bmatrix} 0 \\ 1 \end{bmatrix} \end{array}\right) \tag{6}$$

and generalized for any N_{R} and ratchet design:

$$S_{2\text{-bit}} = \left(\begin{array}{c|c} \mathbb{1}_2 \otimes \begin{bmatrix} \mathbb{1}_{N_{\mathrm{R}}} \\ \mathbb{0}_{N_{\mathrm{R}}} \end{bmatrix} & \mathbb{1}_2 \otimes \begin{bmatrix} \mathbb{0}_{N_{\mathrm{R}}} \\ \mathbb{1}_{N_{\mathrm{R}}} \end{bmatrix} \end{array}\right), \tag{7}$$

$$S_{L\text{-bit}} = \left(\begin{array}{c|c} \mathbb{1}_{2^{L-1}} \otimes \begin{bmatrix} \mathbb{1}_{N_{\mathrm{R}}} \\ \mathbb{0}_{N_{\mathrm{R}}} \end{bmatrix} & \mathbb{1}_{2^{L-1}} \otimes \begin{bmatrix} \mathbb{0}_{N_{\mathrm{R}}} \\ \mathbb{1}_{N_{\mathrm{R}}} \end{bmatrix} \end{array}\right). \tag{8}$$

This completes one cycle of the composite two-step operation $O = SM$, which in general reads

$$O_{L\text{-bit}} = \left(\begin{array}{c|c} \mathbb{1}_{2^{L-1}} \otimes \begin{bmatrix} E \\ G \end{bmatrix} & \mathbb{1}_{2^{L-1}} \otimes \begin{bmatrix} F \\ H \end{bmatrix} \end{array}\right), \tag{9}$$

consisting of a thermal transition step M followed by a switching step S that physically moves the leftmost (output) bit to the right end of the tape.

We highlight a pertinent feature unique to this finite-tape information ratchet not exhibited by its infinite-tape counterparts, i.e., the output bit will eventually return as the input bit in the next *tape* scan once the ratchet has scanned all bits. This allows us to define a *tape* scan operation $(O_{L\text{-bit}})^L$ of L successive *bit* scan operations $O_{L\text{-bit}}$ in the forward spatial direction, previously unattainable in models with an infinite tape. It also provides the mechanism for the system to possibly equilibrate to a steady-state behavior governed by the stationary distribution of $O_{L\text{-bit}}$. This is guaranteed with those matrices O corresponding to *ergodic* finite Markov chains for which O^k has all positive entries for some power $k \in \mathbb{Z}_0^+$, which is also termed as *regular* matrices [36], and we will focus exclusively on such regular O in this paper.

IV. PROOF OF IPSL

We will now embark on proving the IPSL for a general ratchet design with an arbitrary number of bits and ratchet states, which is represented by the probability vector $\mathbf{p}$. The evolution of this vector is governed by the two-step *composite* operation O, i.e.,

$$\mathbf{p}'(\tau) = O\,\mathbf{p}(0). \tag{10}$$

The matrix O physically performs a single bit scan operation and switches to the next input bit, with its dimension determined by the joint tape-ratchet states. For a L-bit tape and N_{R} ratchet states, the size of $O = SM$ is $2^L N_{\mathrm{R}} \times 2^L N_{\mathrm{R}}$, with substeps M and S necessarily having the same dimensions as O.

A. 1-bit tape

For simplicity, we will begin the proof with a 1-bit tape before giving the proof for a tape of arbitrary length L. Note that, for a 1-bit tape, independent of the ratchet design, the switching operation $S_{1\text{-bit}} = \mathbb{1}_{2N_{\mathrm{R}}}$ is the identity matrix which is physically intuitive to understand as the ratchet only interacts with this sole bit throughout its operation.

During *each* thermal transition step M involving the joint single bit-ratchet states, detailed balance is obeyed by the Markovian dynamics. The stochastic transition from state i to state j ($i \to j$) of the joint state is quantified by the transition probability M_{ji}, which is the (j, i) entry of the left stochastic transition matrix M with its columns sum to one due to probability conservation. The detailed balance constraint thus reads

$$M_{ji} p_i^{\text{eq}} = M_{ij} p_j^{\text{eq}} \quad \forall \{i, j\}, \tag{11}$$

where the equilibrium distribution

$$p^{\text{eq}}(x|\beta, \mathbf{E}) = \frac{e^{-\beta E_x}}{\sum_x e^{-\beta E_x}} = \exp\left[\beta(F - E_x)\right] \tag{12}$$

is given by the canonical ensemble in equilibrium statistical mechanics. Note that the system is in contact with a single heat bath, which is responsible for driving the transition between states of different energies, and $F(\beta, \mathbf{E})$ is its Helmholtz free energy. Since the stochastic transitions governing each bit-ratchet interaction are time independent, the transition matrix M and equilibrium distribution $\mathbf{p}^{\text{eq}}$ in Eq. (11) do not have explicit time dependence.

As the ratchet does not retain energy over each operation cycle O ($\Delta E = 0$), energy conservation warrants $\Delta E = \Delta Q = \Delta W$, where ΔQ is the heat transferred into the system and ΔW is the work extracted from the system. This relation applies to every bit for every cycle O. Equations (11) and (12) allow the energy difference $\Delta E_{ji} \equiv E_j - E_i$ to be fixed and expressed as a log ratio of transition probabilities. The expected work production $\langle W \rangle$ from a single transition (bit scan) at any arbitrary time is then given by

$$\langle W \rangle = \sum_{i,\,j} M_{ji} p_i \ln\left(\frac{M_{ij}}{M_{ji}}\right), \tag{13}$$

which is the sum of the respective dimensionless work (originating from thermal transition $i \to j$, with $k_B T = 1$) weighted by the corresponding probability $M_{ji} p_i$ for such a transition to occur.

The switching operation S can be neglected here since only a single bit is involved throughout this ratchet operation so $O_{\text{1-bit}} = M_{\text{1-bit}}$ and this thermal transition step M immediately evolves the distribution $\mathbf{p}(0)$ to $\mathbf{p}'(\tau)$ in each cycle O from Eq. (10).

Next, let us evaluate the change in entropy of the system using the Shannon entropy [37]:

$$\begin{aligned}\Delta H &= H[\mathbf{p}'] - H[\mathbf{p}] = \sum_i p_i \ln p_i - \sum_j p'_j \ln p'_j \\ &= \sum_i \left(\sum_j M_{ji}\right) p_i \ln p_i - \sum_j \left(\sum_i M_{ji} p_i\right) \ln p'_j,\end{aligned} \tag{14}$$

where $\sum_j M_{ji} = 1$ (from probability conservation) is inserted in the first parentheses and the second parentheses results from the action of M on $\mathbf{p}$ (matrix multiplication). Putting the double sums and terms together, the informational term ΔH thus reads

$$\Delta H = \sum_{i,\,j} M_{ji} p_i \ln\left(\frac{p_i}{p'_j}\right). \tag{15}$$

Note that $H[\,\cdot\,]$ is the base 2 binary entropy function but we will use the natural logarithm from hereon to drop the $\ln 2$ factor in the proof.

Now consider the difference between ΔH and $\langle W \rangle$:

$$\Delta H - \langle W \rangle = \sum_{i,\,j} M_{ji} p_i \ln\left(\frac{M_{ji} p_i}{M_{ij} p'_j}\right). \tag{16}$$

The log sum inequality is first applied to the inner sum (within the square brackets) to yield

$$\begin{aligned}\Delta H - \langle W \rangle &= \sum_i p_i \left[\sum_j M_{ji} \ln\left(\frac{M_{ji} p_i}{M_{ij} p'_j}\right)\right] \\ &\geqslant \sum_i p_i \left[\left(\sum_j M_{ji}\right) \ln\left(\frac{\sum_j M_{ji}}{\sum_j \frac{1}{p_i} M_{ij} p'_j}\right)\right] \\ &= \sum_i p_i \ln\left(\frac{p_i}{p''_i}\right),\end{aligned} \tag{17}$$

where we have used $\sum_j M_{ji} = 1$ and $\sum_j M_{ij} p_j^{(n)} = p_i^{(n+1)}$, with the superscript denoting the probability vector after n interactions (bit scans). Applying the log sum inequality once again to the last expression, we obtain

$$\begin{aligned}\Delta H - \langle W \rangle &\geqslant \sum_i p_i \ln\left(\frac{p_i}{p''_i}\right) \geqslant \left(\sum_i p_i\right) \ln\left(\frac{\sum_j p_j}{\sum_k p''_k}\right) \\ &= \ln 1 = 0,\end{aligned} \tag{18}$$

since probability conservation holds at any discrete time. We have thus established our proposed IPSL:

$$\langle W \rangle \leqslant \Delta H. \tag{19}$$

B. >1-bit tape

We emphasize that detailed balance holds for every step M but not O, except for $L = 1$. Another subtle difference relates to the energy levels of the joint states of the equilibrium distribution p^{eq} in Eq. (12); they refer only to the joint interacting bit-ratchet states and not the entire tape with the noninteracting bits. Internal energy thus resides only within the coupled bit-ratchet subsystem. The work expression $\langle W \rangle$, arising from the energy exchanged in the thermal transition of the interacting bit-ratchet joint states, for $L > 1$ is therefore the same as that for $L = 1$ given in Eq. (13). The construction of $M_{L\text{-bit}}$ is such that the transition probabilities in its respective entries will correspond to the same transitions for the 1-bit tape in $M_{\text{1-bit}}$ from Eq. (1). Detailed balance thus holds for each thermal transition step which is independent of L and the different dimensions of $M_{L\text{-bit}}$. As it is the leftmost bit of the tape that interacts with the ratchet physically, it is also possible to express the average work $\langle W \rangle$ in terms of the *marginal interacting bit-ratchet* distribution $\mathbf{p}_{\mathrm{B}_N \otimes \mathrm{R}_N}$, which is shown in the Appendix. It shows that the work expression in terms of this marginal distribution is consistent with the expression as given in Eq. (13) using $M_{L\text{-bit}}$.

However, this $M_{L\text{-bit}}$, $L \neq 1$ acting on an initial probability distribution $\mathbf{p}$ does not yield $\mathbf{p}'$ immediately but an intermediate distribution $\tilde{\mathbf{p}}$, i.e., $M_{L\text{-bit}}\mathbf{p} = \tilde{\mathbf{p}}$. We now see that we require switching S to transform this intermediate $\tilde{\mathbf{p}}$ to $\mathbf{p}'$ at the end of each cycle whose physical operation is to move the detached (leftmost) output bit from the prior thermal transition to the right end of tape. Essentially $S_{L\text{-bit}}$ is a permutation matrix from Eq. (5) and its operation in $\mathbf{p}' = S_{L\text{-bit}}\tilde{\mathbf{p}}$ amounts to reordering the probabilities in $\tilde{\mathbf{p}}$ but leaving the values unchanged. Thus $\tilde{\mathbf{p}}$ and $\mathbf{p}'$ have the same elements and $H[\mathbf{p}'] = H[\tilde{\mathbf{p}}]$, which corresponds to the physical fact that there is no information creation or erasure from this switching operation. In addition, there is no work involved here as the ratchet is not interacting with any bit.

With $\tilde{p}_j = \sum_i M_{ji}p_i$ now for $L > 1$, the expression for ΔH is modified from Eq. (15),

$$\Delta H = \sum_{i,\,j} M_{ji}p_i \ln\left(\frac{p_i}{\tilde{p}_j}\right), \tag{20}$$

and subsequently the difference

$$\Delta H - \langle W\rangle = \sum_{i,\,j} M_{ji}p_i \ln\left(\frac{M_{ji}p_i}{M_{ij}\tilde{p}_j}\right). \tag{21}$$

The proof follows similarly as earlier for $L = 1$ with the application of the log sum inequality in Eq. (17),

$$\begin{aligned}\Delta H - \langle W\rangle &= \sum_i p_i\left[\sum_j M_{ji}\ln\left(\frac{M_{ji}p_i}{M_{ij}\tilde{p}_j}\right)\right]\\ &\geqslant \sum_i p_i\left[\left(\sum_j M_{ji}\right)\ln\left(\frac{\sum_j M_{ji}}{\sum_j \frac{1}{p_i}M_{ij}\tilde{p}_j}\right)\right]\\ &= \sum_i p_i \ln\left(\frac{p_i}{\sum_j M_{ij}\tilde{p}_j}\right),\end{aligned} \tag{22}$$

where we have again used $\sum_j M_{ji} = 1$ (probability conservation). However, the difference stems from the term $\sum_j M_{ij}\tilde{p}_j$, which essentially is an element of another probability distribution since $\tilde{\mathbf{p}} = M\mathbf{p}$ is an intermediate distribution and M is a transition matrix, so $M\tilde{\mathbf{p}} = M^2\mathbf{p}$ is again some probability distribution. Applying the log sum inequality once again, in the same vein as Eq. (18), we obtain the finite-tape IPSL in Eq. (19) from conservation of probability $\sum_i\left(\sum_j M_{ij}\tilde{p}_j\right) = 1$.

This completes the proof of IPSL for finite tapes of all length L.

We also mention the IPSL inequality in (19) saturates [and equivalently the difference $\Delta H - \langle W\rangle$ in Eqs. (16) and (21) vanishes] in the steady-state behavior when the system has converged to its stationary distribution which obeys detailed balance, i.e., in equilibrium. This can be inferred from the arguments of the log terms in Eqs. (16) and (21) and the detailed balance condition in Eq. (11). Conversely, a nonvanishing $\Delta H - \langle W\rangle$ is expected to persist even in steady state as a manifestation of stationary distributions which are not in equilibrium.

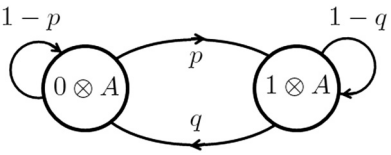

FIG. 3. Transition state diagram for the PC ratchet.

V. PERTURBED COIN (PC) RATCHET

We begin our design and analysis of finite-tape information ratchet with the perturbed coin (PC) model, inspired by [32,33] for simulating stochastic processes. It is the simplest ratchet design with a single ratchet state, and we shall first consider the case for 1-bit finite tape ($L = 1$) to shed light on the underlying single bit-ratchet dynamics before progressing to ratchets with tapes of longer lengths, and also ratchets with multiple states.

A. 1-bit tape

The transition state diagram for the PC ratchet with 1-bit tape is schematically represented in Fig. 3, which has the smallest joint tape-ratchet state space of dimension 2, i.e., $\{0 \otimes A, 1 \otimes A\}$. Note that A is the arbitrary label of the single ratchet state ($N_{\mathrm{R}} = 1$) which we will drop from hereon. The left stochastic transition matrix corresponding to this thermal transition step M is

$$M^{\mathrm{PC}}_{1\text{-bit}} = \begin{array}{c} \\ 0 \\ 1 \end{array}\!\!\begin{array}{c} \begin{array}{cc} 0 & 1 \end{array} \\ \begin{pmatrix} 1-p & q \\ p & 1-q \end{pmatrix} \end{array} = \left(\begin{array}{c|c} E & F \\ \hline G & H \end{array}\right), \tag{23}$$

with transition probabilities $0 \leqslant p, q \leqslant 1$ and its partition labels match those in Eq. (1). For $L = 1$, this $M^{\mathrm{PC}}_{1\text{-bit}} = O^{\mathrm{PC}}_{1\text{-bit}}$ governs the dynamics and is responsible for the evolution of joint single bit-ratchet state probabilities in $\mathbf{p}^{\mathrm{PC}}_{1\text{-bit}}$. Its eigenvalues λ are 1 and $1 - p - q$ with respective right eigenvectors $\boldsymbol{\rho}_1 \equiv \boldsymbol{\pi}^{\mathrm{PC}}_{1\text{-bit}} = \left[\frac{q}{p+q}, \frac{p}{p+q}\right]^{\top}$ and $\boldsymbol{\rho}_{1-p-q} = [1, -1]^{\top}$, with $\boldsymbol{\pi}^{\mathrm{PC}}_{1\text{-bit}}$ (normalized to unity) the invariant or stationary (steady-state) distribution. For an arbitrary initial distribution with the following decomposition

$$\mathbf{p}(0) = a_1\boldsymbol{\pi} + \sum_{|\lambda|<1} a_\lambda \boldsymbol{\rho}_\lambda, \tag{24}$$

this implies with Eq. (10) the following generic expression for a regular O [36]:

$$\mathbf{p}(k) = O^k\,\mathbf{p}(0) = a_1\boldsymbol{\pi} + \sum_{|\lambda|<1} a_\lambda \lambda^k \boldsymbol{\rho}_\lambda. \tag{25}$$

With the corresponding $O^{\mathrm{PC}}_{1\text{-bit}} = M^{\mathrm{PC}}_{1\text{-bit}}$ in Eq. (25) above, the sum (with only one term here: $\lambda = 1 - p - q$ satisfying $|\lambda| < 1$) vanishes, $\lim_{k\to\infty}\mathbf{p}(k) = a_1\boldsymbol{\pi}^{\mathrm{PC}}_{1\text{-bit}}$ and $a_1 = 1$. Here, we are dealing with stationary equilibrium states where the stationary distribution is the equilibrium canonical distribution in Eq. (12), i.e., $\boldsymbol{\pi}^{\mathrm{PC}}_{1\text{-bit}} = \mathbf{p}^{\mathrm{PC,\,eq}}_{1\text{-bit}}$. It also relates the energy levels corresponding to each stochastic transition with the respective extracted work as given in the IPSL proof for 1-bit tape; see Eq. (11).

The necessary and sufficient conditions for convergence are a finite state space and Markovian dynamics, i.e.,

$\mathbf{p}(k+1) = O\,\mathbf{p}(k)$ exhibited by an ergodic Markov chain. Ergodicity here refers to finite Markov chains with all states accessible (irreducible) and acyclic (no periodic distributions); this encompasses those *regular* matrices O which is required to invoke the Perron-Frobenius theorem for a unique and time-independent $\boldsymbol{\pi}$. It is apparent that $O^{\text{PC}}_{\text{1-bit}} = M^{\text{PC}}_{\text{1-bit}}$ satisfies the above conditions for both $p, q \neq 0$ or 1.

It is possible to deduce the analytic expressions of the joint state probabilities p_i between successive transitions:

$$p_0(k) = \frac{q}{p+q} + \left(b - \frac{q}{p+q}\right)(1-p-q)^k, \quad \text{(26a)}$$

$$p_1(k) = \frac{p}{p+q} - \left(b - \frac{q}{p+q}\right)(1-p-q)^k, \quad \text{(26b)}$$

after bit scan k for $k \in \mathbb{Z}_0^+$ for $\mathbf{p}^{\text{PC}}_{\text{1-bit}}(0) = [p_0(0), p_1(0)]^\top$ with $p_0(0) = b$, $p_1(0) = 1-b$, where parameter b can be interpreted as the statistical bias of a "0" in this bit.

Using Eq. (13), the expected work extracted from each *bit* scan (single bit-ratchet interaction) reads

$$\begin{aligned}\langle W\rangle_{k+1} &= \sum_{i,\,j=\{0,1\}} M_{ji}p_i \ln\left(\frac{M_{ij}}{M_{ji}}\right)\\ &= (p+q)\left(b - \frac{q}{p+q}\right)(1-p-q)^k \ln\left(\frac{q}{p}\right)\\ &= [p_0(k) - p_0(k+1)]\cdot W_{0\to 1}, \end{aligned} \quad \text{(27)}$$

where $W_{0\to 1} = \ln(q/p)$ denotes the work done from joint bit-ratchet state 0 to 1. Notice that only transitions between different joint states $0 \leftrightarrow 1$ (and thus with different energies) contribute to the sum since the heat exchanged with the heat reservoir is nonzero. From an information-theoretic perspective, the corresponding change in Shannon entropy of joint distributions over a cycle O is

$$\begin{aligned}\Delta H_{k+1} &= H[\mathbf{p}(k+1)] - H[\mathbf{p}(k)]\\ &= \sum_{i=\{0,1\}} p_i(k)\ln p_i(k) - \sum_{j=\{0,1\}} p_j(k+1)\ln p_j(k+1).\end{aligned} \quad \text{(28)}$$

With Eqs. (27) and (28), we classify this ratchet operation into three distinct regimes [30]: engine (pink) $0 < \langle W\rangle_k \leqslant \Delta H_k$, eraser (blue) $\langle W\rangle_k \leqslant \Delta H_k < 0$, and dud (green) $\langle W\rangle_k \leqslant 0 \leqslant \Delta H_k$, with the corresponding color scheme in Fig. 4 for each bit scan k up to 16 repeated such scans, where the output bit from the preceding bit scan is the input bit for the immediate bit scan since $L = 1$. The respective behaviors can be physically interpreted as follows: engine operation entails (positive) *expected* work extracted from the heat reservoir with the mass raised at the expense of writing information to the distribution of joint single-bit ratchet states (and consuming its memory capacity), erasure behavior erases information within this joint distribution with the expenditure of work (mass lowered), while the dud performs neither useful operation; see [28,29] for similar models.

We can perceive the behaviors described for our finite-tape ratchet as a collective of the assembly of ratchets, and not assertive of the behavior of any single ratchet (specific realization). Thus operating in the engine regime extracts only a positive amount of *expected* work from a random *ensemble* of finite-tape ratchets. On the other hand, erasing information in the finite-tape paradigm refers to decreasing the Shannon entropy of the joint distribution of tape-ratchet states (with work expenditure).

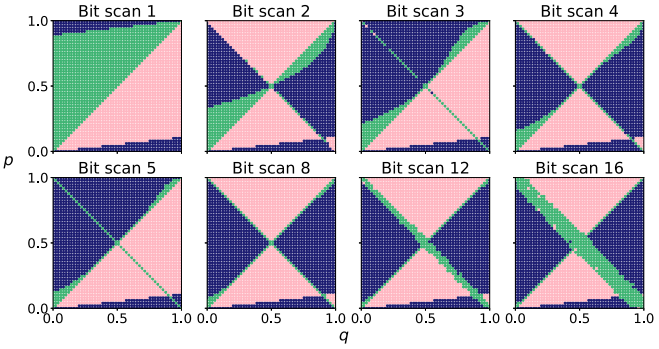

FIG. 4. Phase plots in p-q parameter space (transition probabilities in Fig. 3) of first five bit scans (alternating engine and erasure behaviors above diagonal $p+q=1$) and bit scans 8, 12, and 16 (emergence of eventual dud at this diagonal) for PC ratchet with 1-bit tape starting in initial distribution $\mathbf{p}^{\text{PC}}_{\text{1-bit}}(0) = [p_0(0), p_1(0)]^\top = [b, 1-b]^\top$ ($b = 0.9$) denoting the different operation regimes: engine (pink; the lightly shaded region), eraser (blue; the most darkly shaded region), and dud (green; the intermediate shaded region), which all satisfy the IPSL in Eq. (46).

It is easy to see that $\langle W\rangle_k \to 0$, $\Delta H_k \to 0$ as $k \to \infty$ respectively from the term $(1-p-q)^k$ with $|1-p-q| < 1$ and $\mathbf{p}^{\text{PC}}_{\text{1-bit}}(k)$ converging to $\boldsymbol{\pi}^{\text{PC}}_{\text{1-bit}}$. The p-q phase plot will thus be eventually dominated by the dud regime as the system equilibrates with no useful expected work to be drawn further. In Fig. 4, the top-left to bottom-right diagonal line $p+q=1$ are (p,q) points where the eigenvalue $|\lambda| < 1$ vanishes and the rate of convergence is the fastest from Eq. (25). This is responsible for the emergence of a dud region originating from this line where $\langle W\rangle_k$ becomes vanishingly small and approaches zero.[1] Above the diagonal ($p+q > 1$), the sign of $\langle W\rangle_k$ alternates between successive scans from $(1-p-q)^k$, which brings about an interchanging engine and erasure behavior.

This interesting feature, where the same (p,q) can support various operation regimes in different bit or tape scans performed successively, may confer flexibility to a user operating the finite-tape ratchet as a means to switch modalities, although the ratchet could be unreliable in sustaining a single mode of operation.

As we run the PC ratchet, the magnitude of $\langle W\rangle_k$ diminishes for successive k from Eq. (27), i.e., $|\langle W\rangle_{k+1}| \leqslant |\langle W\rangle_k|$. We thus expect the *cumulative* expected work $\sum_k \langle W\rangle_k$ to have the same sign as $\langle W\rangle_1$ from the first bit scan even though individual bit scans may suggest an alternating engine and

[1] Both $\langle W\rangle_k$ and ΔH_k can only approach close to zero at long time and numerical errors potentially throw up misleading cases of IPSL violation. We address this by classifying ratchet behavior based on their signs in Fig. 4: opposite signs for dud and same signs (both positive for engine and both negative for eraser), since our IPSL proof shows that these violations are not mathematically possible.

erasure behavior noted earlier from the phase plots in Fig. 4. Summing $\langle W\rangle_k$ in Eq. (27), the *cumulative* expected work reads

$$\sum_{k=1}^{\infty}\langle W\rangle_k = (p+q)\left(b-\frac{q}{p+q}\right)\ln\left(\frac{q}{p}\right)\sum_{k=1}^{\infty}(1-p-q)^{k-1} = \left(b-\frac{q}{p+q}\right)\ln\left(\frac{q}{p}\right) = [p_0(0)-\pi_0]\cdot W_{0\to 1}. \tag{29}$$

Depending on the intended objectives, a user equipped with the PC ratchet may thus choose to operate the finite-tape ratchet either once to extract a *one-shot* (expected) work $\langle W\rangle_1$ or over multiple bit scans to leverage the *cumulative* (expected) work $\sum_k\langle W\rangle_k$ depending on the parameter settings $p+q\lesseqgtr 1$ and knowledge of Fig. 4 to determine the signs of successive $\langle W\rangle_k$.

B. >1-bit tape

Next, let us generalize to a PC ratchet with L-bit tape by first taking $L=2$ as an example. We consider an initial 2-bit tape with joint distribution $\mathbf{p}^{\mathrm{PC}}_{\text{2-bit}}(0)=[p_{00}(0),p_{01}(0),p_{10}(0),p_{11}(0)]^{\top}$, where we have again dropped the single ratchet state in the labels. As the ratchet interacts with each bit sequentially, the *marginal interacting bit-ratchet* distribution $\mathbf{p}_{\mathrm{B}_N\otimes\mathrm{R}_N}$ from the joint tape-ratchet distribution $\mathbf{p}$ determines the work $\langle W\rangle$ in each bit scan operation; see the Appendix for further details. For the single-state PC ratchet, essentially $\mathbf{p}^{\mathrm{PC}}_{\mathrm{B}_N\otimes\mathrm{R}_N}=\mathbf{p}^{\mathrm{PC}}_{\mathrm{B}_N}$ since $N_{\mathrm{R}}=1$ and we can thus characterize $\mathbf{p}^{\mathrm{PC}}_{\mathrm{B}_i}(b_i)$ with its respective bias b_i to be a "0" bit, independent of the other bits in the tape.

The required thermal transition step here is

$$M^{\mathrm{PC}}_{\text{2-bit}} = \begin{array}{c} \\ \underline{0}\underline{0} \\ \underline{0}\underline{1} \\ \underline{1}\underline{0} \\ \underline{1}\underline{1} \end{array}\!\!\begin{array}{c} \begin{array}{cccc} \underline{0}\underline{0} & \underline{0}\underline{1} & \underline{1}\underline{0} & \underline{1}\underline{1} \end{array} \\ \begin{pmatrix} 1-p & 0 & q & 0 \\ 0 & 1-p & 0 & q \\ p & 0 & 1-q & 0 \\ 0 & p & 0 & 1-q \end{pmatrix} \end{array}, \tag{30}$$

followed by a switching operation given earlier in Eq. (5) which then leads to the two-step *single bit* scan operation $O=SM$:

$$O^{\mathrm{PC}}_{\text{2-bit}} = \begin{array}{c} \\ \underline{0}\underline{0} \\ \underline{0}\underline{1} \\ \underline{1}\underline{0} \\ \underline{1}\underline{1} \end{array}\!\!\begin{array}{c} \begin{array}{cccc} \underline{0}\underline{0} & \underline{0}\underline{1} & \underline{1}\underline{0} & \underline{1}\underline{1} \end{array} \\ \begin{pmatrix} 1-p & 0 & q & 0 \\ p & 0 & 1-q & 0 \\ 0 & 1-p & 0 & q \\ 0 & p & 0 & 1-q \end{pmatrix} \end{array}. \tag{31}$$

Since $M^{\mathrm{PC}}_{L\text{-bit}}\neq O^{\mathrm{PC}}_{L\text{-bit}}$ for $L>1$, we need to check the regularity of $O^{\mathrm{PC}}_{L\text{-bit}}$ for one complete bit scan and not just for the thermal transition $M^{\mathrm{PC}}_{L\text{-bit}}$ to determine possible convergence. We see that $O^{\mathrm{PC}}_{\text{2-bit}}$ is also a regular matrix so $\mathbf{p}^{\mathrm{PC}}_{\text{2-bit}}(0)$ will converge to $\boldsymbol{\pi}^{\mathrm{PC}}_{\text{2-bit}}=\left[\frac{q^2}{(p+q)^2},\frac{qp}{(p+q)^2},\frac{pq}{(p+q)^2},\frac{p^2}{(p+q)^2}\right]^{\top}=\boldsymbol{\pi}^{\mathrm{PC},(1)}_{\text{1-bit}}\otimes\boldsymbol{\pi}^{\mathrm{PC},(2)}_{\text{1-bit}}$ and exhibit identical long-term behavior as the 1-bit tape. This applies to all $O^{\mathrm{PC}}_{L\text{-bit}}$ due to their ergodicity and similarly for all $\mathbf{p}^{\mathrm{PC}}_{L\text{-bit}}(0)$. Its eventual convergence can be generalized as

$$\lim_{k\to\infty}\mathbf{p}^{\mathrm{PC}}_{L\text{-bit}}(k)=\boldsymbol{\pi}^{\mathrm{PC}}_{L\text{-bit}}=\bigotimes_{i=1}^{L}\boldsymbol{\pi}^{\mathrm{PC},(i)}_{\text{1-bit}}. \tag{32}$$

This follows from the independent *marginal* bit distributions $\mathbf{p}^{\mathrm{PC}}_{\mathrm{B}_i}(b_i)$ which explain the independent individual bit-ratchet interactions. Crucially, the single state of the PC ratchet is responsible for the lack of correlation between the bit stream and itself, which it is unable to generate and introduce from its operation.

Unlike an information ratchet harvesting work out of an infinite bit sequence, our finite-tape version squeezes work out of the information in the tape through repeated *tape* scans. In other words, it continues to act on the output bits from the previous bit scan operations which circulate back to the ratchet after *all bits in the finite tape* have been scanned in the preceding tape scan. The involved *bit* scan work $\langle W\rangle$ and *tape* scan work $\langle W_{\mathrm{t}}\rangle$ are mathematically related by

$$\langle W_{\mathrm{t}}\rangle_k=\sum_{i=1}^{L}\langle W^{(i)}\rangle_k, \tag{33}$$

i.e., the work from *tape* scan k is the sum of the respective *bit* scan works from the kth *bit* scan of *all* bits in an L-bit finite tape. For $L=1$, $\langle W_{\mathrm{t}}\rangle_k=\langle W\rangle_k$ and there is no distinction between *bit* and *tape* scan work. For $L>1$, as the bits interact with the PC ratchet independently, the bias b_i from the marginal distribution of each bit B_i (again neglecting the sole ratchet state; in general, $\mathrm{B}_i\otimes\mathrm{R}$) is a parameter of $\langle W^{(i)}\rangle(b_i)$ for a fixed (p,q) and from the individual *bit* scan work in Eq. (27),

$$\langle W_{\mathrm{t}}\rangle^{\mathrm{PC}}_k=\sum_{i=1}^{L}(p+q)\left(b_i-\frac{q}{p+q}\right)(1-p-q)^{k-1}\ln\left(\frac{q}{p}\right) = \left(\sum_{i=1}^{L}C_i(b_i)\right)(1-p-q)^{k-1}, \tag{34}$$

where $C_i(b_i)=(p+q)[b_i-q/(p+q)]\ln(q/p)$ is introduced to make the decay of $\langle W_{\mathrm{t}}\rangle^{\mathrm{PC}}_k$ manifestly apparent. The *cumulative* tape scan work after N tape scans is thus

$$\sum_{k=1}^{N}\langle W_{\mathrm{t}}\rangle^{\mathrm{PC}}_k=\left(\sum_{i=1}^{L}C_i(b_i)\right)\sum_{k=1}^{N}(1-p-q)^{k-1} = \left(\sum_{i=1}^{L}C_i(b_i)\right)\frac{[1-(1-p-q)^N]}{p+q}. \tag{35}$$

C. Maximizing $\sum_k\langle W\rangle_k$

We seek to obtain the maximal work from the information ratchet with tapes of different length L to study the effect of different ratchet designs. For this, we will need to optimize over a range of parameters such as the initial distribution $\mathbf{p}(0)$ and the transition probability M_{ij}. For our finite-tape information ratchet, we would like to optimize over the cumulative work $\sum_k\langle W\rangle_k$. Note that

$$\sum_{k=1}^{\infty}\langle W_{\mathrm{t}}\rangle_k=\sum_{k=1}^{\infty}\sum_{i=1}^{L}\langle W^{(i)}\rangle_k=\sum_{k=1}^{\infty}\langle W\rangle_k, \tag{36}$$

where $\langle W\rangle_k$ represents the expected work for bit scan k, i.e., Eq. (27) for the PC ratchet. Therefore, it is the same optimizing over the bit scan work or the tape scan work.

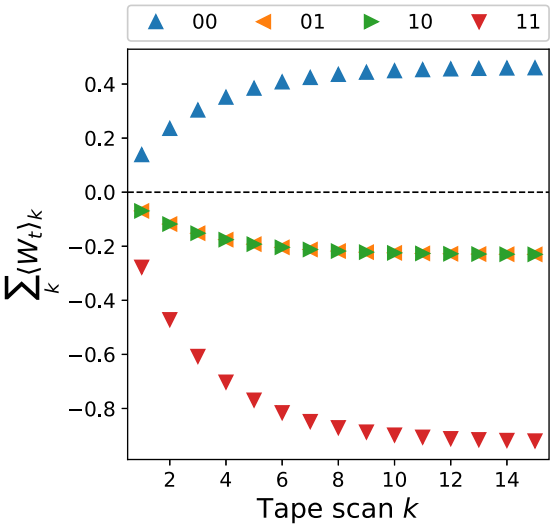

FIG. 5. Plot of respective cumulative tape scan work $\sum_k \langle W_t \rangle_k$ for PC ratchet with 2-bit tape starting in the definite-state joint (tape-ratchet) distributions [corresponding to (joint tape-ratchet) states 00, 01, 10, and 11] at fixed transition probabilities $(p, q) = (0.1,\ 0.2)$.

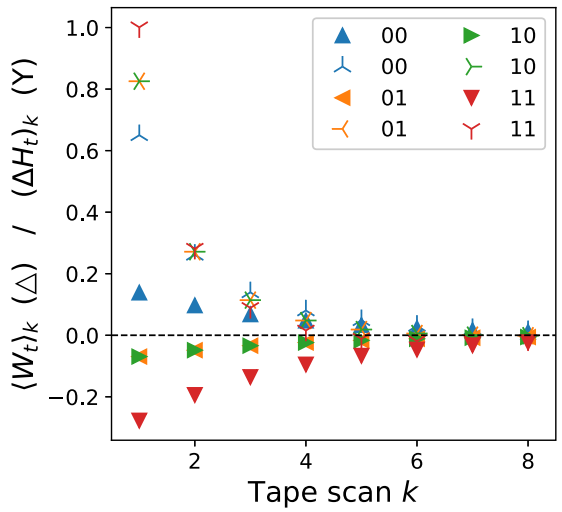

FIG. 6. Plot of respective tape scan work $\langle W_t \rangle_k$ (in △) with corresponding upper bound $\langle \Delta H_t \rangle_k$ (in Y), the change in Shannon entropy of its joint (tape-ratchet) distribution over tape scan k, for PC ratchet with 2-bit tape starting in the definite-state joint (tape-ratchet) distributions in Fig. 5, i.e., joint states 00, 01, 10, and 11, at fixed transition probabilities $(p, q) = (0.1,\ 0.2)$.

Based on Eqs. (10) and (13), we have

$$\langle W \rangle_k = \mathbf{p}(0)^\top \left(O^\top\right)^{k-1} \mathbf{W}, \tag{37}$$

where $\mathbf{W}$ is a vector of size $2^L N_R \times 1$ with elements given by $W_i = \sum_j M_{ji} W_{i\to j}$ with $W_{i\to j} = \ln(M_{ij}/M_{ji})$, ordered in a corresponding manner to $\mathbf{p}(0)$. Note that $\top$ represents the transpose operation. The cumulative work is then given by

$$\begin{aligned}\sum_{k=1}^{\infty} \langle W \rangle_k &= \sum_{k=1}^{\infty} \mathbf{p}(0)^\top \left(O^\top\right)^{k-1} \mathbf{W} \\ &= \mathbf{p}(0)^\top \left[\sum_{k=1}^{\infty} \left(O^\top\right)^{k-1} \mathbf{W}\right] \\ &= \mathbf{p}(0)^\top \mathbf{W}', \end{aligned} \tag{38}$$

where the element W_i' of

$$\mathbf{W}' = \sum_{k=1}^{\infty} \left(O^\top\right)^{k-1} \mathbf{W} \tag{39}$$

gives the cumulative work when the initial probability of the joint tape-ratchet distribution $\mathbf{p}(0)$ has element $p_i = 1$ with the rest of its elements zero. We call such a joint distribution the definite-state joint distribution.

Our results in Eqs. (38) and (39) imply the following. The maximal cumulative work occurs as the maximum of the elements of $\mathbf{W}'$. According to Eq. (38), any combination of the elements in $\mathbf{p}(0)$ will lead to a cumulative work less than this maximum except for $p_i = 1$ and $p_{j\neq i} = 0$ when the maximum is W_i'.

Thus, for the PC 2-bit tape, we need to ascertain which of the following initial definite-state joint distributions: $[1, 0, 0, 0]^\top$, $[0, 1, 0, 0]^\top$, $[0, 0, 1, 0]^\top$, and $[0, 0, 0, 1]^\top$ for the joint tape-ratchet states 00, 01, 10, and 11, respectively, gives the maximum cumulative work. Figure 5 presents the cumulative tape scan work $\sum_k \langle W_t \rangle_k^{\mathrm{PC}}$ from these distributions for an arbitrarily chosen $(p, q) = (0.1,\ 0.2)$. It is evident that the distribution for 00, i.e., $[1, 0, 0, 0]^\top$, yields the maximum cumulative work. This distribution would also maximize over all the other possible initial probability distributions of $\mathbf{p}_{2\text{-bit}}^{\mathrm{PC}}(0)$ for the cumulative work when $(p, q) = (0.1,\ 0.2)$, since the work is simply a sum of W_i' weighted by the respective initial probabilities p_i in $\mathbf{p}_{2\text{-bit}}^{\mathrm{PC}}(0)$ as discussed above.

We also present the respective upper bounds $\langle \Delta H_t \rangle_k$, i.e., the change in Shannon entropy of its corresponding joint distribution over tape scan k in Fig. 6, noting $\langle W_t \rangle_k \to 0$, $\langle \Delta H_t \rangle_k \to 0$ with $k \to \infty$. Their difference $\langle \Delta H_t \rangle_k - \langle W_t \rangle_k$ vanishes, implying the steady-state behavior of these initial definite-state joint distributions (in Fig. 5) are all in equilibrium and saturate the IPSL inequality [over 1 bit scan in the proof (19) and equivalently tape scan here]. The corresponding stationary distributions thus satisfy detailed balance in Eq. (11).

After maximizing over $\mathbf{p}(0)$ for fixed transition matrix elements, the next optimization step is to maximize over the transition matrix elements (transition probabilities). For the PC 2-bit tape, the maximization is performed over the parameters p and q and we have employed the basin-hopping algorithm [38] for this purpose. The maximal work $\sum_k \langle W \rangle_k$ and corresponding optimized (p, q) will be presented subsequently in Tables I and II for further discussion.

VI. MODIFIED BOYD'S (MB) RATCHET

A. 1-bit tape

We have modified Boyd's (MB) original ratchet design [30] by including new transitions parametrized by ϵ, where $0 < \epsilon < 1$, in order to ensure that its thermal transition matrix M is regular (Fig. 7). It has two possible ratchet states (arbitrarily labeled A, B) with corresponding transition matrix for

TABLE I. Maximal cumulative tape scan work $\langle W\rangle_{\max} = \max\left(\sum_k \langle W_t\rangle_k\right)$ for PC and MB ($\epsilon = 0.9$) ratchets over 300 tape scans with finite tapes of different length L and the corresponding second largest eigenvalue $|\lambda_{2\text{nd}}|$ of the tape scan operation matrix $(O_{L\text{-bit}})^L$ characterizing the convergence rate.

L-bit	$\langle W\rangle^{\text{PC}}_{\max}$	$\langle W\rangle^{\text{MB}}_{\max}$	$\lvert\lambda^{\text{PC}}_{2\text{nd}}\rvert$	$\lvert\lambda^{\text{MB}}_{2\text{nd}}\rvert$
1-bit	0.27846	0.59868	0.26568	0.91124
2-bit	0.55693	0.82838	0.26568	0.84338
3-bit	0.83539	1.10624	0.54441	0.81785
4-bit	1.11386	1.38440	0.14303	0.80903
5-bit	1.39232	1.66269	0.26568	0.80380
6-bit	1.67079	1.94105	0.44540	0.80027

$L = 1$:

$$M^{\text{MB}}_{1\text{-bit}} = \begin{array}{c} \\ 0\otimes A \\ 0\otimes B \\ 1\otimes A \\ 1\otimes B \end{array} \begin{array}{c} \begin{array}{cccc} 0\otimes A & 0\otimes B & 1\otimes A & 1\otimes B \end{array} \\ \begin{pmatrix} \epsilon & 1-p & 0 & 0 \\ 1-\epsilon & 0 & q & 0 \\ 0 & p & 0 & 1-\epsilon \\ 0 & 0 & 1-q & \epsilon \end{pmatrix} \end{array}, \tag{40}$$

which doubles the joint tape-ratchet space for all finite L-bit tapes. This ratchet design allows for the possibility of generating correlation between bits and ratchet from their interaction since the ratchet now also possesses memory. Previously for the PC ratchet without memory, only the tape (of bits) possesses memory where one approach outlined in [28,29] attributed the tape as a "memory register" (with memory).

This perspective of conferring memory to the ratchet, dependent on the number of its ratchet states N_{R}, is inspired by Boyd in [30,32,34], where he employed the framework of computational mechanics (the study of patterns and structures in the organization of complex systems) to associate the ratchet states with its causal states in the construction of its hidden Markov model (HMM). Although we are not pursuing his approach in our paper, we have nonetheless adopted the perspective of both the tape and ratchet (with $N_{\text{R}} > 1$) possessing memory whose rationale is based on the earlier analogy.

TABLE II. Respective optimal transition probabilities $(p_{\max}, q_{\max})$ corresponding to the maximal cumulative tape scan work $\langle W\rangle_{\max}$ in Table I for PC and MB ratchets with tapes of different length L.

L-bit	$p^{\text{PC}}_{\max}$	$q^{\text{PC}}_{\max}$	$p^{\text{MB}}_{\max}$	$q^{\text{MB}}_{\max}$
1-bit	0.99000	0.27568	0.87606	0.59303
2-bit	0.99000	0.27568	0.71039	0.96507
3-bit	0.35636	0.09923	0.96451	0.71548
4-bit	0.89406	0.24896	0.71831	0.96417
5-bit	0.27568	0.99000	0.72012	0.96395
6-bit	0.12080	0.43380	0.72137	0.96380

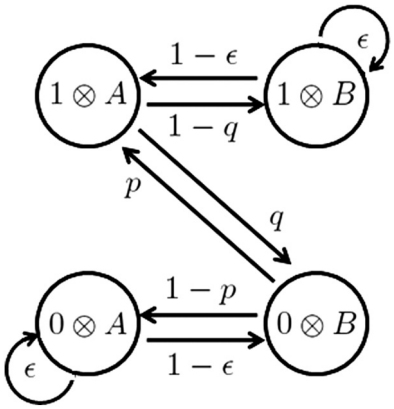

FIG. 7. Transition state diagram for modified Boyd's ratchet.

We will restrict our discussion to the general case $\epsilon \neq 0$, in which all initial distributions $\mathbf{p}^{\text{MB}}_{1\text{-bit}}(0)$ will converge to

$$\boldsymbol{\pi}^{\text{MB}}_{1\text{-bit}}(\epsilon) = [2(p+q-pq)-(p+q)\epsilon]^{-1}\begin{pmatrix}(1-p)q\\(1-\epsilon)q\\(1-\epsilon)p\\p(1-q)\end{pmatrix}, \tag{41}$$

which is the right eigenvector of $O^{\text{MB}}_{1\text{-bit}}(\epsilon) = M^{\text{MB}}_{1\text{-bit}}(\epsilon)$ in Eq. (40) with eigenvalue 1, and $\langle W\rangle$, $\Delta H \to 0$ since $M^{\text{MB}}_{1\text{-bit}}(\epsilon \neq 0)$ is regular. Similar to PC ratchet, its eventual behavior is all dud but the convergence rates differ according to the eigenvalues of their respective $O_{1\text{-bit}}$, which we will discuss further subsequently.

In the case of the original ratchet of Boyd *et al.* with $\epsilon = 0$, the ratchet always alternates between states A and B, possibly leading to an eventual periodic joint probability distribution. Convergence to a stationary distribution $\boldsymbol{\pi}^{\text{MB}}_{1\text{-bit}}$ is not guaranteed since $O^{\text{MB}}_{1\text{-bit}}(\epsilon = 0)$ is irregular, and similarly for all $O^{\text{MB}}_{L\text{-bit}}(\epsilon = 0)$ with this ratchet design. We will thus not be exploring this case here because our focus is on ergodic and regular O in this paper.

B. 2-bit tape

Explicitly, $M^{\text{MB}}_{L\text{-bit}}$ can be constructed with Eq. (4) by using the respective blocks from $M^{\text{MB}}_{1\text{-bit}}$ in Eq. (40) and similarly for $O^{\text{MB}}_{L\text{-bit}}$ with Eq. (9). It is instructive now to proceed to the 2-bit tape (again for $\epsilon \neq 0$) to reveal how tape-ratchet correlation can manifest within this system and its implications on the resulting dynamics, specifically work production.

For $O^{\text{MB}}_{2\text{-bit}}(\epsilon \neq 0)$ which is regular here, all initial joint distributions $\mathbf{p}^{\text{MB}}_{2\text{-bit}}(0)$ will converge to

$$\boldsymbol{\pi}^{\text{MB}}_{2\text{-bit}}(\epsilon) = (\cdots)\begin{pmatrix}(1-p)q^2\epsilon(2-p-\epsilon)\\q^2\epsilon(1-\epsilon)(2-p-\epsilon)\\pq(1-\epsilon)[p+q-p(q+\epsilon)]\\pq\epsilon(1-\epsilon)(2-q-\epsilon)\\pq\epsilon(1-\epsilon)(2-p-\epsilon)\\pq(1-\epsilon)[p+q-q(p+\epsilon)]\\p^2\epsilon(1-\epsilon)(2-q-\epsilon)\\p^2(1-q)\epsilon(2-q-\epsilon)\end{pmatrix}, \tag{42}$$

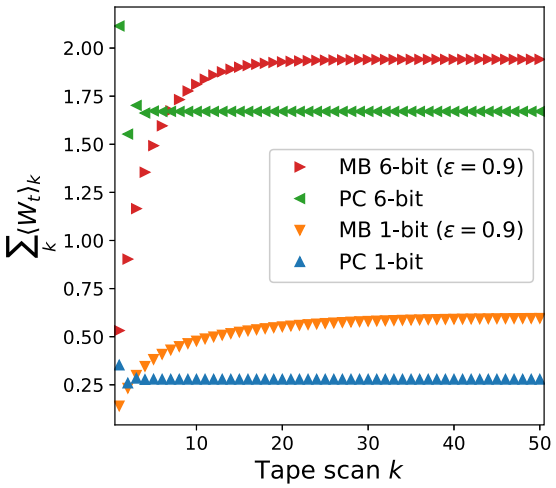

FIG. 8. Plot of respective maximal cumulative tape scan work $\sum_k \langle W_t \rangle_k$ for PC and MB ratchets with 1-bit and 6-bit tapes separately over 50 tape scans. The maximization is performed over the corresponding initial joint distributions $\mathbf{p}(0)$ and transition probabilities (p, q) with the additional parameter $\epsilon = 0.9$ fixed in MB ratchet. The respective upper bounds $(\Delta H_t)_k$, the change in Shannon entropy of the corresponding joint distribution over tape scan k, are presented with the tape scan work $\langle W_t \rangle_k$ in Figs. 9 and 10 to illustrate their steady-state behavior which saturates the IPSL in Eq. (19). The tape scan work $\langle W_t \rangle_k$ is also separately fitted to an exponential model in Figs. 11 and 12 to determine the respective time constants: $\tilde{\tau}^{\text{PC}}_{\text{1-bit}} = 0.75445$, $\tilde{\tau}^{\text{MB}}_{\text{1-bit}} = 10.75732$ for $L = 1$ and $\tilde{\tau}^{\text{PC}}_{\text{6-bit}} = 1.23643$, $\tilde{\tau}^{\text{MB}}_{\text{6-bit}} = 4.36301$ for $L = 6$.

with normalization

$$(\cdots) = \Big\{\epsilon[p^2(2-q-\epsilon)^2 + q^2(2-p-\epsilon)^2] + 2pq(1-\epsilon)[p+q-pq+\epsilon(2-p-q-\epsilon)]\Big\}^{-1}. \tag{43}$$

Notice the 2 bits are coupled in a sense that their marginal distributions $\mathbf{p}^{\text{MB}}_{\text{B}_N \otimes \text{R}_N}$ are not independent but tied with the nontrivial ratchet state (unlike in PC ratchet). However, its eventual behavior will similarly be all dud for such regular matrices $O^{\text{MB}}_{\text{2-bit}}(\epsilon \neq 0)$, whose convergence to $\boldsymbol{\pi}^{\text{MB}}_{\text{2-bit}}(\epsilon \neq 0)$ is guaranteed from their ergodicity.

VII. COMPARISON OF PC AND MB RATCHETS

We now perform a comparison between the PC and MB ratchet designs presented earlier in terms of their work production in their respective engine regimes. We seek their respective maximal cumulative tape scan work $\sum_k \langle W_t \rangle_k$ to quantify which design is best leveraged and utilized for work extraction. Similar to the earlier methodology for PC ratchet, we maximize this work from operating the MB ratchet over its respective set of definite-state joint distributions, for a fixed (p, q) first before optimizing over different (p, q), to facilitate this comparison and present the effect of $N_{\text{R}} \geqq 1$ (presence or absence of ratchet memory) on the maximal work. Moreover, we would also need to optimize over the additional ϵ parameter in the MB ratchet. Because we found that $\sum_k \langle W_t \rangle_k$ approaches a maximum when $\epsilon \to 1$, we fix it at a regime where it gives large $\sum_k \langle W_t \rangle_k$. Hence we set $\epsilon = 0.9$.

The respective $\langle W \rangle_{\max} = \max(\sum_k \langle W_t \rangle_k)$ from PC and MB ratchets with finite tapes of different length L (after 300 tape scans) is presented in Table I, with the corresponding set

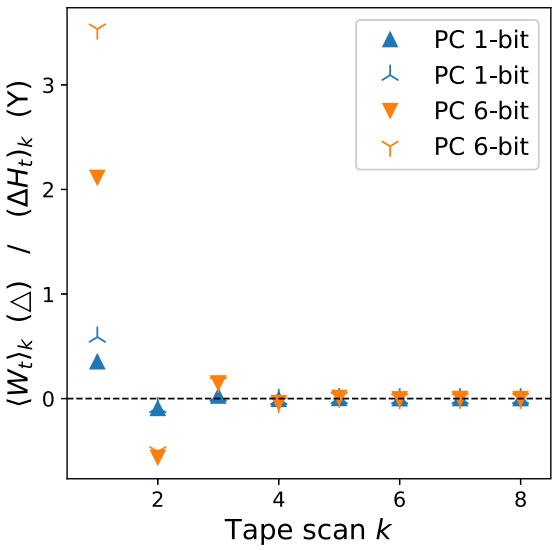

FIG. 9. Plot of respective tape scan work $\langle W_t \rangle_k$ (in △) with corresponding upper bound $(\Delta H_t)_k$ (in Y), the change in Shannon entropy of its joint (tape-ratchet) distribution over tape scan k, for PC ratchet with 1-bit and 6-bit tapes starting separately in the respective definite-state joint distribution, which maximizes the cumulative work in Fig. 8 with the optimal transition probabilities $(p_{\max}, q_{\max})$ in Table II.

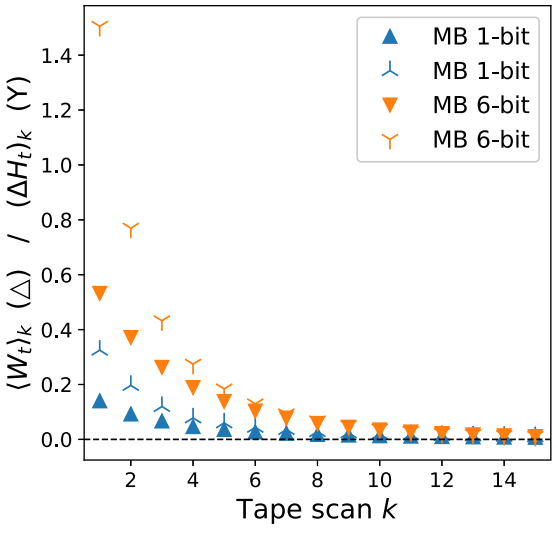

FIG. 10. Plot of respective tape scan work $\langle W_t \rangle_k$ (in △) with corresponding upper bound $(\Delta H_t)_k$ (in Y), the change in Shannon entropy of its joint (tape-ratchet) distribution over tape scan k, for MB ratchet ($\epsilon = 0.9$) with 1-bit and 6-bit tapes starting separately in the respective definite-state joint distribution, which maximizes the cumulative work in Fig. 8 with the optimal transition probabilities $(p_{\max}, q_{\max})$ in Table II.

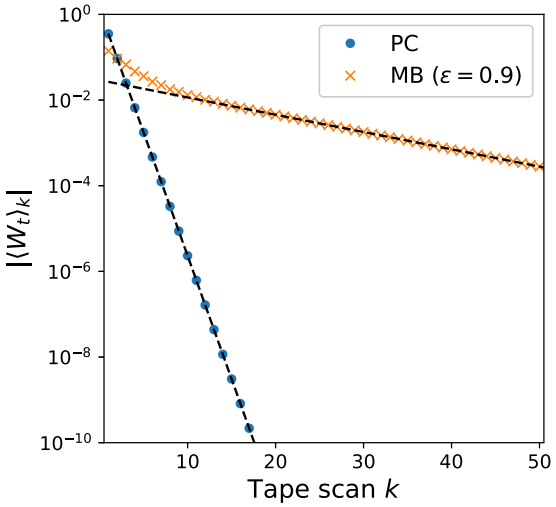

FIG. 11. Semilog plot of magnitude of respective tape scan work $|\langle W_t \rangle_k|$ for PC and MB ratchets with 1-bit tape (optimized in Fig. 8). The black dotted line is a fitting of $|\langle W_t \rangle_k|$ to an exponential function $|\langle W_t \rangle_k| = ab^k$, with fitted parameters given in Table III.

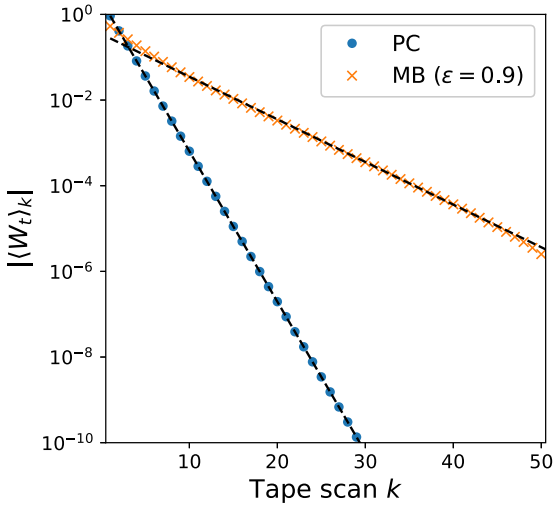

FIG. 12. Semilog plot of magnitude of respective tape scan work $|\langle W_t \rangle_k|$ for PC and MB ratchets with 6-bit tape (optimized in Fig. 8). The black dotted line is a fitting of $|\langle W_t \rangle_k|$ to an exponential function $|\langle W_t \rangle_k| = ab^k$, with fitted parameters given in Table III.

of optimized parameters in Table II. This work in general increases with the length L of finite tape, which is physically intuitive as more work can potentially be leveraged from more bits within a longer tape with a larger memory capacity as a thermodynamic resource. More importantly, we note the advantage conferred by MB ratchet in terms of $\langle W \rangle_{\max}$ extracted for all $1 \leqslant L \leqslant 6$ explored numerically here, which suggests the MB ratchet design is more suited for the sole purpose of harnessing the maximal work from a given limited resource (finite tape). For $L = 1$ and $L = 6$, the numerically obtained cumulative work $\sum_k \langle W_t \rangle_k$ for $\langle W \rangle_{\max}$ is plotted for both PC and MB ratchets in Fig. 8 to illustrate their convergent behaviors and evaluate their sustainability as a thermodynamic engine. We note the numerical $\sum_k \langle W_t \rangle_k^{\rm PC}$ matches with the analytic expression in Eq. (35).

It is intriguing that these parameters, which yield the maximal cumulative tape scan work $\sum_k \langle W_t \rangle_k$, lead to a steady-state behavior (when the system has converged to its stationary distribution) in equilibrium with $\langle W_t \rangle_k \to 0$, $(\Delta H_t)_k \to 0$ in Figs. 9 and 10 and the difference in Eqs. (16) and (21) vanishes, saturating the IPSL inequality in (19). These stationary distributions thus satisfy detailed balance given in Eq. (11). However, a quick comparison between Figs. 9 and 10 reveals a difference in convergence rates for the PC and MB ratchets, which we will now analyze further.

The eigenvalues of the respective *tape* scan operations O^L govern the decay of the *tape* scan work $\langle W_t \rangle_k$ from Eqs. (24) and (25) in the earlier analysis with repeated applications of O^L acting on the joint tape-ratchet distribution $\mathbf{p}$ successively in every *tape* scan. Regular matrices with dimension d necessarily have an eigenvalue $\lambda = 1$ corresponding to the stationary distribution (eigenvector) $\boldsymbol{\pi}$ with the remaining $d - 1$ eigenvalues having magnitudes $|\lambda| < 1$. The largest (in terms of magnitude) of these $d - 1$ eigenvalues, $\lambda_{2\rm nd}$ is responsible for the asymptotic decay rate of tape scan work $\langle W_t \rangle_k$ as $\mathbf{p}$ converges to $\boldsymbol{\pi}$ at equilibrium with contributions from the other eigenvalues (i.e., $\lambda \neq 1$ or $\lambda \neq \lambda_{2\rm nd}$) vanishing first.

We begin this analysis with the PC ratchet for 1-bit tape, where the eigenvalues of $O^{\rm PC}_{\text{1-bit}} = M^{\rm PC}_{\text{1-bit}}$ are $\lambda^{\rm PC}_{\text{1-bit}} = 1$, $1 - p - q$; thus the sums in Eqs. (24) and (25) have only one term and $(\lambda^{\rm PC}_{\text{1-bit}})_{2\rm nd} = 1 - p - q$ with $|(\lambda^{\rm PC}_{\text{1-bit}})_{2\rm nd}| < 1$. From the tape scan work $\langle W_t \rangle_k^{\rm PC}$ in Eq. (34) and equivalently bit scan work since $L = 1$ in Eq. (27), it indeed has an exponential decay governed by this $(\lambda^{\rm PC}_{\text{1-bit}})_{2\rm nd}$, which we can linearize as

$$\ln \left| \langle W_t \rangle_k^{\rm PC} \right| = \ln \left| \sum_{i=1}^{L} C_i(b_i) \right| + (k-1) \ln |1 - p - q|, \quad (44)$$

with slope $\ln |1 - p - q| < 0$ in a logarithmic plot of the magnitude of tape scan work $|\langle W_t \rangle_k^{\rm PC}|$ with tape scan k. In addition, it can be deduced that $\lambda^{\rm PC}_{\rm 2nd} = 1 - p - q \; \forall L$ from Eq. (34). For $L > 1$, there are other nondominant eigenvalues (with magnitudes smaller than $\lambda^{\rm PC}_{\rm 2nd}$) whose contributions to the decay of $\langle W_t \rangle_k^{\rm PC}$ vanish at long time. The plots for $L = 1$ and $L = 6$ (on a semilog scale) in Figs. 11 and 12 are consistent with this analysis as the calculated $|\lambda^{\rm PC}_{\rm 2nd}| = |1 - p^{\rm PC}_{\max} - q^{\rm PC}_{\max}|$ [by using the optimized $(p^{\rm PC}_{\max}, q^{\rm PC}_{\max})$ in Table II] matches with the numerically obtained $|\lambda^{\rm PC}_{\rm 2nd}|$ as the second largest (in magnitude) eigenvalue of $(O^{\rm PC}_{L\text{-bit}})^L$, and also with the fitted

TABLE III. Respective parameters (a, b) obtained from the fitting of tape scan work in Figs. 11 and 12 for PC and MB (with first 30 tape scans omitted) ratchets with L-bit tape ($L = 1$, 6) to an exponential function $|\langle W_t \rangle_k| = ab^k$. Transition probabilities used to obtain $\langle W_t \rangle_k$ correspond to $\langle W \rangle_{\max}$ in Table I and given in Table II. The fitted parameters have negligible errors from the fitting. Note the good agreement between the fitted b and the corresponding $|\lambda_{2\rm nd}|$ in Table I.

L-bit	$a^{\rm PC}$	$b^{\rm PC}$	$a^{\rm MB}$	$b^{\rm MB}$
1-bit	1.32659	0.26568	0.02917	0.91123
6-bit	2.08043	0.44540	0.34724	0.79517

parameter b^{PC} from the fitting to the exponential function $|\langle W_{\mathrm{t}}\rangle_k| = ab^k$; see Table III.

Similarly for the MB ratchet, we pursue a similar approach and conjecture that its $\langle W_{\mathrm{t}}\rangle_k^{\mathrm{MB}}$ also follows an exponential decay governed by its eigenvalues $\{\lambda_{L\text{-bit}}^{\mathrm{MB}} \neq 1\}$ of $(O_{L\text{-bit}}^{\mathrm{MB}})^L$. We present similar plots in Figs. 11 and 12, and we omit the first 30 tape scans in the fitting of $\langle W_{\mathrm{t}}\rangle_k^{\mathrm{MB}}$ to obtain a more accurate estimate of $|\lambda_{2\mathrm{nd}}^{\mathrm{MB}}|$ with b^{MB} given in Table III. The reason is that, with $\dim(O_{1\text{-bit}}^{\mathrm{MB}}) = 4$, there are three eigenvalues responsible for the decay of $\langle W_{\mathrm{t}}\rangle_k^{\mathrm{MB}}$. The initial transients at small k are a manifestation of the other nondominant eigenvalues, specifically the smallest two (in magnitude) which do not contribute to the long term decay of the tape scan work $\langle W_{\mathrm{t}}\rangle_k^{\mathrm{MB}}$.

We can quantify the convergence of $\langle W_{\mathrm{t}}\rangle_k$ with its $\lambda_{2\mathrm{nd}}$ by calculating the respective time constant $\tilde{\tau}$ from the exponential function recasted as

$$|\langle W_{\mathrm{t}}\rangle_k| = ab^k = a\,\exp\left[-\frac{k}{-(\ln b)^{-1}}\right] = a\,e^{-k/\tilde{\tau}}, \qquad (45)$$

and noting $b = |\lambda_{2\mathrm{nd}}|$ so $\tilde{\tau}$ can be found either from $\tilde{\tau} = -(\ln|\lambda_{2\mathrm{nd}}|)^{-1}$ using $\lambda_{2\mathrm{nd}}$, the second largest (in magnitude) eigenvalue of O^L in Table I, or $\tilde{\tau} = -(\ln b)^{-1}$ using the fitted b in Table II. Since our earlier results showed good agreement between the fitted b and the corresponding $\lambda_{2\mathrm{nd}}$, either method will give us the time constant: $\tilde{\tau}_{L\text{-bit}}^{\mathrm{PC}}$, $\tilde{\tau}_{L\text{-bit}}^{\mathrm{MB}}$ for $L = 1$ and $L = 6$ in Fig. 8 explicitly. It is apparent that $\tilde{\tau}^{\mathrm{MB}} > \tilde{\tau}^{\mathrm{PC}}$ for $0 \leqslant L \leqslant 6$ and the MB ratchet has a prolonged utility as an engine over the PC ratchet from our numerical investigation.

Thus we surmize that the MB ratchet fares better than the PC ratchet both in terms of total cumulative work extraction and sustainability as a thermodynamic engine, where it has a longer time constant and hence a slower convergence rate, towards equilibrium.

VIII. CONCLUSION

In conclusion, we have established an information processing second law (IPSL) for a *finite-tape* information ratchet as follows:

$$\langle W\rangle \leqslant k_B T\ \ln 2(H[\mathbf{p}'] - H[\mathbf{p}]). \qquad (46)$$

It is analogous to the original IPSL introduced by Boyd *et al.* [30] for an infinite sequence of bits:

$$\langle W\rangle \leqslant k_B T\ \ln 2\,(h'_\mu - h_\mu), \qquad (47)$$

where the time-averaged work production rate $\langle W\rangle$ of the ratchet in its steady-state behavior is bounded above by the change in entropy rate $\Delta h_\mu = h'_\mu - h_\mu$. Unlike the infinite tape version, our finite tape-ratchet system takes the perspective of an *ensemble* of information ratchets operating on their respective finite tapes, where we study and explore their collective or ensemble-averaged behavior. Each member of the information ratchet ensemble is identical (in terms of its design, e.g., number of ratchet states, permissible state transitions with respective transition probabilities) and operates on its finite tape (all of the same length) within this ensemble, and as such could be perceived as a random machine. Hence Eq. (46) is to be interpreted as the ensemble-averaged (expected) work $\langle W\rangle$ being bounded by the change in Shannon entropy between the resulting $\mathbf{p}'$ and preceding $\mathbf{p}$ joint distributions over the tape-ratchet configurations over an arbitrary time step (1 bit scan), irrespective of whether the initial transients have passed or eventual convergence to a stationary distribution. This is a fundamental difference between the infinite-tape IPSL and the finite-tape IPSL with the latter's applicability at all times, resulting in a different interpretation for the work term in the respective inequalities: a steady-state, time-averaged work production rate in Eq. (47) and an ensemble-averaged (expected) work extracted for a particular bit scan in Eq. (46). We note that information now manifests within the joint distribution of the configuration (joint states) of the tape-ratchet system at a specific time, in stark contrast with Boyd *et al.*'s model where the explicit (input and output) bit sequences are the stores of information.

We studied the potential of this finite-tape information ratchet in fulfilling the thermodynamic role of supporting a variety of ratchet operations with two ratchet designs in this paper: a single-state, perturbed coin ratchet and double-state, modified Boyd's ratchet. We found that the finiteness of the tape renders the useful operation of engine or eraser unsustainable in time as the system equilibrates under the action of regular O matrices with no useful (i.e., positive) expected work to be extracted or expended further after prolonged operation. Nonetheless, the ratchet is still able to realize its utility as either an engine (positive work extracted at the expense of writing information to the joint tape-ratchet distribution) or eraser (work expended for information erasure within this joint distribution), respectively, under different sets of parameters in its transient phase before equilibrium has been attained. Specifically, knowledge of the phase plots such as Fig. 4 will equip a user operating this random machine with the corresponding (p, q) parameters to leverage its expected behavior (either as an engine or eraser) to complete the desired physical tasks of generating and extracting work or information erasure.

Finally, we show how correlation can be harnessed to extract additional cumulative work. Through our design, we illustrate that an information ratchet with memory draws more cumulative work relative to another without by exploiting correlations between ratchet state and bit state in view of the presence of ratchet memory. Moreover, the effect of tape-ratchet correlations when $N_{\mathrm{R}} > 1$ can bias a ratchet with memory away from equilibrium such that its asymptotic tape scan work $\langle W_{\mathrm{t}}\rangle_\infty$ is nonvanishing. We have uncovered this phenomenon for the MB ratchet for $L > 1$ at specific (p, q) values where the steady state $\langle W_{\mathrm{t}}\rangle_\infty^{\mathrm{MB}}$ is observed to exhibit a negative value. With the system having converged to its stationary distribution $\mathbf{p} \to \boldsymbol{\pi}$, the change in Shannon entropy of its joint distribution (over a bit scan and thus a tape scan) vanishes, i.e., $(\Delta H_{\mathrm{t}})_\infty = 0$. In accordance with the IPSL in Eq. (46) and taking into account the negative work in this steady state, we observe that $(\Delta H_{\mathrm{t}})_\infty - \langle W_{\mathrm{t}}\rangle_\infty > 0$. This exemplifies the situation where the nonsaturation of the IPSL inequality persists in the steady state when the system is not in equilibrium. To understand these results, further investigation on the underlying mechanism behind how the ratchet leverage and exploit correlated joint tape-ratchet distributions to maximize the extracted work from its continued operation is necessary. We believe such

exploration in our future work would lead us to the design of finite-tape information ratchets that realize exotic or self-sustaining thermodynamic functionalities.

APPENDIX: WORK AND MARGINAL PROBABILITY DISTRIBUTION

Here we show that the average work $\langle W\rangle$ for the $L>1$-bit tape can be expressed in terms of the *marginal interacting bit-ratchet* distribution. In order to do this, some new indexing notations will be introduced, starting from the 1-bit tape operation first and then the general L-bit tape operation.

1. 1-bit tape

The thermal transition operator for the 1-bit tape is given by Eq. (1) where E, F, G, and H are submatrices of $M_{\text{1-bit}}$ with size $N_{\text{R}}\times N_{\text{R}}$. To ease the notation later, here we refer to $M_{\text{1-bit}}$ as $M^{(1)}$. We refer to the entry or element of $M^{(1)}$ as $M^{(1)}_{i,j}$.

Let us now define new variables r, s, u, and v, where $r,s\in\{0,1\}$ and $u,v\in\{1,2,\ldots,N_{\text{R}}\}$. The indices i and j can then be defined as

$$i(r,u)=rN_{\text{R}}+u, \tag{A1}$$

$$j(s,v)=sN_{\text{R}}+v. \tag{A2}$$

The variables r and s determine which submatrix the indices are referring to, i.e.,

$$\begin{aligned} E &\rightarrow r=0,\quad s=0,\\ F &\rightarrow r=0,\quad s=1,\\ G &\rightarrow r=1,\quad s=0,\\ H &\rightarrow r=1,\quad s=1, \end{aligned} \tag{A3}$$

and the variables u and v refer to the row and column of the particular submatrix, respectively.

Following Eq. (13), the average work can be written in terms of r, s, u, and v as

$$\begin{aligned}\langle W\rangle &= \sum_{i,j} M^{(1)}_{j,i}p_i \ln\left(\frac{M^{(1)}_{i,j}}{M^{(1)}_{j,i}}\right)\\ &= \sum_{r=0}^{1}\sum_{s=0}^{1}\sum_{u=1}^{N_{\text{R}}}\sum_{v=1}^{N_{\text{R}}} M^{(1)}_{(sN_{\text{R}}+v,\,rN_{\text{R}}+u)}p_{(rN_{\text{R}}+u)}\\ &\quad\times\ln\left[\frac{M^{(1)}_{(rN_{\text{R}}+u,\,sN_{\text{R}}+v)}}{M^{(1)}_{(sN_{\text{R}}+v,\,rN_{\text{R}}+u)}}\right]. \end{aligned} \tag{A4}$$

As for the probability distribution $p_i=p_{(rN_{\text{R}}+u)}$, Table IV gives the relationship among the variables r and u, index i, and the corresponding tape-ratchet configurations for $N_{\text{R}}=2$.

2. L-bit tape

The thermal transition operator for the L-bit tape $M^{(L)}$ is given by Eq. (4). Each of the submatrices E, F, G, and H in $M^{(L)}$ is repeated 2^{L-1} times. Outside of these submatrices, all other elements of $M^{(L)}$ are zero.

TABLE IV. Relationship among the variables r and u, index i, and the tape-ratchet configuration for $N_{\text{R}}=2$.

r	u	i	Tape-ratchet configuration
0	1	1	$0\otimes A$
0	2	2	$0\otimes B$
1	1	3	$1\otimes A$
1	2	4	$1\otimes B$

Since there are repeating elements of submatrices E, F, G, and H in $M^{(L)}$, variables r, s, u, and v introduced before can be used again here to refer to the elements of these submatrices. Let us now define new variables k, α, and β, where $k\in\{0,1,\ldots,2^{L-1}-1\}$ and

$$\alpha(r,u,k)=rN_{\text{R}}2^{L-1}+kN_{\text{R}}+u, \tag{A5}$$

$$\beta(s,v,k)=sN_{\text{R}}2^{L-1}+kN_{\text{R}}+v. \tag{A6}$$

It can be checked that $M^{(L)}_{\alpha,\beta}=M^{(1)}_{i,j}$ (and $M^{(L)}_{\beta,\alpha}=M^{(1)}_{j,i}$) for any k. The variables r and s can be thought of pointing to the *region* of the matrix $M^{(L)}$, as shown below:

$$M^{(L)}=\left(\begin{array}{c|c} r=0,s=0 & r=0,s=1\\ \hline r=1,s=0 & r=1,s=1\end{array}\right). \tag{A7}$$

Additionally, the variables r and s also determine which submatrix the indices are referring to, as given in Eq. (A3). Variable k points to the $(k+1)$th copy of the submatrix, counting from top to bottom (or left to right). Since k can take 2^{L-1} different values, it indicates that the repetition of the elements occurs 2^{L-1} times. The variables u and v refer to the row and column of the particular submatrix, respectively.

The elements of $M^{(L)}$ outside of indices α and β defined above are all zero. Therefore, the average work as expressed in Eq. (13) can be calculated by summing over the indices α and β, i.e.,

$$\begin{aligned}\langle W\rangle &= \sum_{\alpha,\beta} M^{(L)}_{\beta,\alpha}p_\alpha \ln\left(\frac{M^{(L)}_{\alpha,\beta}}{M^{(L)}_{\beta,\alpha}}\right)\\ &= \sum_{r=0}^{1}\sum_{s=0}^{1}\sum_{u=1}^{N_{\text{R}}}\sum_{v=1}^{N_{\text{R}}}\sum_{k=0}^{2^{L-1}-1} M^{(L)}_{(sN_{\text{R}}2^{L-1}+kN_{\text{R}}+v,\,rN_{\text{R}}2^{L-1}+kN_{\text{R}}+u)}\\ &\quad\times p_{(rN_{\text{R}}2^{L-1}+kN_{\text{R}}+u)}\\ &\quad\times\ln\left[\frac{M^{(L)}_{(rN_{\text{R}}2^{L-1}+kN_{\text{R}}+u,\,sN_{\text{R}}2^{L-1}+kN_{\text{R}}+v)}}{M^{(L)}_{(sN_{\text{R}}2^{L-1}+kN_{\text{R}}+v,\,rN_{\text{R}}2^{L-1}+kN_{\text{R}}+u)}}\right]. \end{aligned} \tag{A8}$$

Since $M^{(L)}_{\alpha,\beta}=M^{(1)}_{i,j}$ and $M^{(L)}_{\beta,\alpha}=M^{(1)}_{j,i}$, then $M^{(L)}_{(rN_{\text{R}}2^{L-1}+kN_{\text{R}}+u,\,sN_{\text{R}}2^{L-1}+kN_{\text{R}}+v)}=M^{(1)}_{(rN_{\text{R}}+u,\,sN_{\text{R}}+v)}$ and $M^{(L)}_{(sN_{\text{R}}2^{L-1}+kN_{\text{R}}+v,\,rN_{\text{R}}2^{L-1}+kN_{\text{R}}+u)}=M^{(1)}_{(sN_{\text{R}}+v,\,rN_{\text{R}}+u)}$. Therefore,

$$\begin{aligned}\langle W\rangle &= \sum_{r=0}^{1}\sum_{s=0}^{1}\sum_{u=1}^{N_{\text{R}}}\sum_{v=1}^{N_{\text{R}}} M^{(1)}_{(sN_{\text{R}}+v,\,rN_{\text{R}}+u)}\\ &\quad\times\left[\sum_{k=0}^{2^{L-1}-1} p_{(rN_{\text{R}}2^{L-1}+kN_{\text{R}}+u)}\right] \end{aligned}$$

TABLE V. Relationship among the variables r, u, k, the indices i and α, and the tape-ratchet configuration for $N_{\mathrm{R}} = 2$ and $L = 2$.

r	k	u	α	Tape-ratchet configuration	i
0	0	1	1	$00 \otimes A$	1
0	0	2	2	$00 \otimes B$	2
0	1	1	3	$01 \otimes A$	1
0	1	2	4	$01 \otimes B$	2
1	0	1	5	$10 \otimes A$	3
1	0	2	6	$10 \otimes B$	4
1	1	1	7	$11 \otimes A$	3
1	1	2	8	$11 \otimes B$	4

$$\times \ln\left[\frac{M^{(1)}_{(rN_{\mathrm{R}}+u,\, sN_{\mathrm{R}}+v)}}{M^{(1)}_{(sN_{\mathrm{R}}+v,\, rN_{\mathrm{R}}+u)}}\right] = \sum_{i,j} M^{(1)}_{j,i} p^{(\mathrm{B}_N \otimes \mathrm{R}_N)}_{i(r,u)} \ln\left(\frac{M^{(1)}_{i,j}}{M^{(1)}_{j,i}}\right), \tag{A9}$$

where $p^{(\mathrm{B}_N \otimes \mathrm{R}_N)}_{i(r,u)}$ is the marginal probability defined as

$$p^{(\mathrm{B}_N \otimes \mathrm{R}_N)}_{i(r,u)} = \sum_{k=0}^{2^{L-1}-1} p_{(rN_{\mathrm{R}}2^{L-1}+kN_{\mathrm{R}}+u)}. \tag{A10}$$

So Eq. (A9) shows that the average work can be calculated from the marginals following the exact same formulation as the 1-bit tape's average work.

Table V gives the relationship among the variables r, u, k, the indices i and α, and the corresponding tape-ratchet configurations for $N_{\mathrm{R}} = 2$ and $L = 2$. The list of the marginals in this example is given by

$$\begin{aligned} p_{(0\otimes A)} &= p_1 + p_3 = p_{(00\otimes A)} + p_{(01\otimes A)}, \\ p_{(0\otimes B)} &= p_2 + p_4 = p_{(00\otimes B)} + p_{(01\otimes B)}, \\ p_{(1\otimes A)} &= p_5 + p_7 = p_{(10\otimes A)} + p_{(11\otimes A)}, \\ p_{(1\otimes B)} &= p_6 + p_8 = p_{(10\otimes B)} + p_{(11\otimes B)}. \end{aligned} \tag{A11}$$

[1] *Maxwell's Demon 2 Entropy, Classical and Quantum Information, Computing*, edited by H. Leff and A. F. Rex (CRC Press, Boca Raton, FL, 2002).

[2] K. Maruyama, F. Nori, and V. Vedral, Colloquium: The physics of Maxwell's demon and information, Rev. Mod. Phys. **81**, 1 (2009).

[3] R. Landauer, Irreversibility and heat generation in the computing process, IBM J. Res. Dev. **5**, 183 (1961).

[4] L. Szilard, On the decrease of entropy in a thermodynamic system by the intervention of intelligent beings, Behav. Sci. **9**, 301 (1964).

[5] C. E. Shannon, A mathematical theory of communication, Bell Syst. Tech. J. **27**, 379 (1948).

[6] E. T. Jaynes, Information theory and statistical mechanics, Phys. Rev. **106**, 620 (1957).

[7] E. T. Jaynes, Information theory and statistical mechanics. II, Phys. Rev. **108**, 171 (1957).

[8] C. H. Bennett, The thermodynamics of computation—a review, Int. J. Theor. Phys. **21**, 905 (1982).

[9] C. Jarzynski, Equalities and inequalities: Irreversibility and the second law of thermodynamics at the nanoscale, Annu. Rev. Condens. Matter Phys. **2**, 329 (2011).

[10] S. Deffner and C. Jarzynski, Information Processing and the Second Law of Thermodynamics: An Inclusive, Hamiltonian Approach, Phys. Rev. X **3**, 041003 (2013).

[11] K. Sekimoto, *Stochastic Energetics* (Springer, Berlin, 2010).

[12] U. Seifert, Stochastic thermodynamics, fluctuation theorems and molecular machines, Rep. Prog. Phys. **75**, 126001 (2012).

[13] A. Barato and U. Seifert, Unifying Three Perspectives on Information Processing in Stochastic Thermodynamics, Phys. Rev. Lett. **112**, 090601 (2014).

[14] A. C. Barato and U. Seifert, Stochastic thermodynamics with information reservoirs, Phys. Rev. E **90**, 042150 (2014).

[15] T. Sagawa, *Thermodynamics of Information Processing in Small Systems* (Springer, Japan, 2013).

[16] T. Sagawa and M. Ueda, Information thermodynamics: Maxwell's demon in nonequilibrium dynamics, in *Nonequilibrium Statistical Physics of Small Systems* (Wiley-VCH Verlag GmbH & Co. KGaA, Berlin, 2013), pp. 181–211.

[17] J. M. R. Parrondo, J. M. Horowitz, and T. Sagawa, Thermodynamics of information, Nat. Phys. **11**, 131 (2015).

[18] G. Schaller, C. Emary, G. Kiesslich, and T. Brandes, Probing the power of an electronic Maxwell's demon: Single-electron transistor monitored by a quantum point contact, Phys. Rev. B **84**, 085418 (2011).

[19] A. Bérut, A. Arakelyan, A. Petrosyan, S. Ciliberto, R. Dillenschneider, and E. Lutz, Experimental verification of Landauer's principle linking information and thermodynamics, Nature (London) **483**, 187 (2012).

[20] J. Koski, V. Maisi, T. Sagawa, and J. Pekola, Experimental Observation of the Role of Mutual Information in the Nonequilibrium Dynamics of a Maxwell Demon, Phys. Rev. Lett. **113**, 030601 (2014).

[21] J. V. Koski, V. F. Maisi, J. P. Pekola, and D. V. Averin, Experimental realization of a szilard engine with a single electron, Proc. Natl. Acad. Sci. USA **111**, 13786 (2014).

[22] M. D. Vidrighin, O. Dahlsten, M. Barbieri, M. Kim, V. Vedral, and I. A. Walmsley, Photonic Maxwell's Demon, Phys. Rev. Lett. **116**, 050401 (2016).

[23] J. M. Horowitz and S. Vaikuntanathan, Nonequilibrium detailed fluctuation theorem for repeated discrete feedback, Phys. Rev. E **82**, 061120 (2010).

[24] J. M. Horowitz and J. M. R. Parrondo, Thermodynamic reversibility in feedback processes, Europhys. Lett. **95**, 10005 (2011).

[25] J. M. Horowitz and J. M. R. Parrondo, Designing optimal discrete-feedback thermodynamic engines, New J. Phys. **13**, 123019 (2011).

[26] F. J. Cao and M. Feito, Thermodynamics of feedback controlled systems, Phys. Rev. E **79**, 041118 (2009).

[27] T. Sagawa and M. Ueda, Generalized Jarzynski Equality under Nonequilibrium Feedback Control, Phys. Rev. Lett. **104**, 090602 (2010).

[28] D. Mandal and C. Jarzynski, Work and information processing in a solvable model of Maxwell's demon, Proc. Natl. Acad. Sci. USA **109**, 11641 (2012).

[29] D. Mandal, H. T. Quan, and C. Jarzynski, Maxwell's Refrigerator: An Exactly Solvable Model, Phys. Rev. Lett. **111**, 030602 (2013).

[30] A. B. Boyd, D. Mandal, and J. P. Crutchfield, Identifying functional thermodynamics in autonomous Maxwellian ratchets, New J. Phys. **18**, 023049 (2016).

[31] J. Hoppenau and A. Engel, On the energetics of information exchange, Europhys. Lett. **105**, 50002 (2014).

[32] A. B. Boyd, D. Mandal, and J. P. Crutchfield, Leveraging environmental correlations: The thermodynamics of requisite variety, J. Stat. Phys. **167**, 1555 (2017).

[33] F. Ghafari, N. Tischler, C. D. Franco, J. Thompson, M. Gu, and G. J. Pryde, Interfering trajectories in experimental quantum-enhanced stochastic simulation, Nat. Commun. **10**, 1630 (2019).

[34] A. B. Boyd, D. Mandal, and J. P. Crutchfield, Correlation-powered information engines and the thermodynamics of self-correction, Phys. Rev. E **95**, 012152 (2017).

[35] G. E. Crooks, Path-ensemble averages in systems driven far from equilibrium, Phys. Rev. E **61**, 2361 (2000).

[36] J. P. Sethna, *Statistical Mechanics: Entropy, Order Parameters, and Complexity* (Oxford University Press, Oxford, 2021).

[37] T. M. Cover and T. J. A, *Elements of Information Theory*, 2nd ed. (John Wiley & Sons, New York, 2006).

[38] D. J. Wales and J. P. K. Doye, Global optimization by basin-hopping and the lowest energy structures of Lennard-Jones clusters containing up to 110 atoms, J. Phys. Chem. A **101**, 5111 (1997).